

**U-Load
Dextramer®**

Build multimers with your choice of peptide and peptide-receptive MHC I and MHC II alleles.



This information is current as of February 24, 2022.

Neutrophil and Granulocytic Myeloid-Derived Suppressor Cell-Mediated T Cell Suppression Significantly Contributes to Immune Dysregulation in Common Variable Immunodeficiency Disorders

Marcela Vlkova, Zita Chovancova, Jana Nechvatalova, Ashley Nicole Connelly, Marcus Darrell Davis, Peter Slanina, Lucie Travnickova, Marek Litzman, Tereza Grymova, Premysl Soucek, Tomas Freiburger, Jiri Litzman and Zdenek Hel

J Immunol 2019; 202:93-104; Prepublished online 28 November 2018;

doi: 10.4049/jimmunol.1800102

<http://www.jimmunol.org/content/202/1/93>

Supplementary Material <http://www.jimmunol.org/content/suppl/2018/11/27/jimmunol.1800102.DCSupplemental>

References This article **cites 70 articles**, 18 of which you can access for free at: <http://www.jimmunol.org/content/202/1/93.full#ref-list-1>

Why *The JI*? Submit online.

- **Rapid Reviews! 30 days*** from submission to initial decision
- **No Triage!** Every submission reviewed by practicing scientists
- **Fast Publication!** 4 weeks from acceptance to publication

**average*

Subscription Information about subscribing to *The Journal of Immunology* is online at: <http://jimmunol.org/subscription>

Permissions Submit copyright permission requests at: <http://www.aai.org/About/Publications/JI/copyright.html>

Email Alerts Receive free email-alerts when new articles cite this article. Sign up at: <http://jimmunol.org/alerts>

The Journal of Immunology is published twice each month by
The American Association of Immunologists, Inc.,
1451 Rockville Pike, Suite 650, Rockville, MD 20852
Copyright © 2018 by The American Association of
Immunologists, Inc. All rights reserved.
Print ISSN: 0022-1767 Online ISSN: 1550-6606.



Neutrophil and Granulocytic Myeloid-Derived Suppressor Cell-Mediated T Cell Suppression Significantly Contributes to Immune Dysregulation in Common Variable Immunodeficiency Disorders

Marcela Vlkova,^{*,†} Zita Chovancova,^{*,†} Jana Nechvatalova,^{*,†} Ashley Nicole Connelly,^{‡,§} Marcus Darrell Davis,^{‡,§} Peter Slanina,^{*,†} Lucie Travnickova,^{*} Marek Litzman,[¶] Tereza Grymova,^{||,¶} Premysl Soucek,^{||,¶} Tomas Freiburger,^{*,||,¶} Jiri Litzman,^{*,†} and Zdenek Hel^{‡,§}

Common variable immunodeficiency disorders (CVID) represent a group of primary immunodeficiency diseases characterized by hypogammaglobulinemia and impaired specific Ab response, resulting in recurrent infections due to dysfunctional immune response. The specific mechanisms mediating immune deficiency in CVID remain to be determined. Previous studies indicated that immune dysregulation in CVID patients is associated with chronic microbial translocation, systemic immune activation, and altered homeostasis of lymphocytic and myeloid lineages. A detailed phenotypic, functional characterization of plasma markers and immune cell populations was performed in 46 CVID patients and 44 healthy donors. CVID patients displayed significantly elevated plasma levels of a marker of neutrophil activation neutrophil gelatinase-associated lipocalin. Neutrophils from CVID patients exhibited elevated surface levels of CD11b and PD-L1 and decreased levels of CD62L, CD16, and CD80, consistent with a phenotype of activated neutrophils with suppressive properties. Neutrophils from CVID patients actively suppressed T cell activation and release of IFN- γ via the production of reactive oxygen species. Furthermore, CVID was associated with an increased frequency of low-density neutrophils (LDNs)/granulocytic myeloid-derived suppressor cells. LDN/granulocytic myeloid-derived suppressor cell frequency in CVID patients correlated with reduced T cell responsiveness. Exogenous stimulation of whole blood with bacterial LPS emulated some but not all of the phenotypic changes observed on neutrophils from CVID patients and induced neutrophil population with LDN phenotype. The presented data demonstrate that neutrophils in the blood of CVID patients acquire an activated phenotype and exert potent T cell suppressive activity. Specific targeting of myeloid cell-derived suppressor activity represents a novel potential therapeutic strategy for CVID. *The Journal of Immunology*, 2019, 202: 93–104.

Common variable immunodeficiency disorders (CVID) are a heterogeneous group of defects representing the most frequent form of primary symptomatic hypogammaglobulinemia (1). CVID patients suffer from clinically significant immunodeficiency that manifests by frequent and severe respiratory tract infections, diarrhea, and autoimmune disorders. Recurrent bacterial infections in CVID patients are predominantly caused by *Streptococcus pneumoniae*, *Haemophilus influenzae*, and *Staphylococcus aureus* (2, 3). In ~2–10% of patients with CVID, specific mutations in more than 20 genes were described,

including genes coding for LPS-responsive beige-like anchor protein (LRBA), CTLA-4, CD19, CD20, CD21, CD81, ICOS, BAFF-R, transmembrane activator and calcium modulator and cyclophilin ligand interactor (TACI), and others (2, 3). Previous studies have demonstrated a number of lymphocytic abnormalities in CVID patients, including chronic T cell activation, reduced T cell functionality, and decreased absolute numbers of CD4⁺ T cells and NK cells in the systemic circulation (4–10). The specific mechanisms underlying systemic immune dysregulation in CVID remain unclear. Studies by others and us demonstrated

*Department of Clinical Immunology and Allergology, Faculty of Medicine, Masaryk University, 625 00 Brno, Czech Republic; [†]St. Anne's University Hospital, 656 91 Brno, Czech Republic; [‡]Department of Pathology, University of Alabama at Birmingham, Birmingham, AL 35249; [§]Department of Microbiology, University of Alabama at Birmingham, Birmingham, AL 35294; [¶]Department of Economics, Faculty of Business and Economics, Mendel University in Brno, 613 00 Brno, Czech Republic; ^{||}Central European Institute of Technology, Masaryk University, 601 77 Brno, Czech Republic; and [¶]Centre for Cardiovascular Surgery and Transplantation, 656 91 Brno, Czech Republic

ORCID: 0000-0003-2122-7784 (M.V.); 0000-0003-0634-005X (J.N.); 0000-0003-3257-487X (A.N.C.); 0000-0003-0076-3668 (P. Slanina); 0000-0002-1332-3103 (L.T.); 0000-0001-9495-8188 (M.L.); 0000-0002-9985-2531 (P. Soucek); 0000-0001-6532-7053 (T.F.).

Received for publication January 23, 2018. Accepted for publication October 26, 2018.

This work was supported by Grant 15-28732A from the Czech Ministry of Health.

Address correspondence and reprint requests to Dr. Marcela Vlkova, Department of Clinical Immunology and Allergology, Faculty of Medicine, St Anne's University Hospital and Faculty of Medicine, Masaryk University, Pekarska 53, 656 91 Brno, Czech Republic. E-mail address: marcela.vlkova@fnusa.cz

The online version of this article contains supplemental material.

Abbreviations used in this article: CAT, catalase; CVID, common variable immunodeficiency disorder; G-MDSC, granulocytic myeloid-derived suppressor cell; iNOS, inducible NO synthase; LDN, low-density neutrophil; L-NHA, *N*^G-hydroxy-L-arginine monoacetate; L-NMMA, *N*^ω-monomethyl-L-arginine acetate salt; NGAL, neutrophil gelatinase-associated lipocalin; ROS, reactive oxygen species, sCD14, soluble CD14; SOD, superoxide dismutase; SSC, side light scatter.

Copyright © 2018 by The American Association of Immunologists, Inc. 0022-1767/18/\$37.50

that immune dysregulation in CVID is associated with chronic microbial translocation, systemic activation of myeloid cells, and altered phenotype of myeloid cell-derived cytokines, including increased production of G-CSF and other factors involved in granulopoiesis and regulation of neutrophil recruitment and activation (10–13).

Neutrophils represent the most abundant nucleated leukocyte population (50–70% of all WBCs) that is specifically geared for sensitive detection of bacterial products (14–16). Any significant functional alteration of this population is likely to exert a profound effect on the host. Systemic bacterial or viral infection induces a hematopoietic response referred to as emergency granulopoiesis, with up to 1×10^{11} granulocytes generated each day (17, 18). Recent elegant studies have demonstrated that emergency granulopoiesis is driven by G-CSF produced by endothelial cells in response to LPS signaling via TLR4/MyD88 pathway (18–20). G-CSF-induced neutrophils were shown to arise from alternative differentiation pathway from common myeloid progenitors and granulocyte/macrophage progenitors, produce reactive oxygen species (ROS), and display potent immunosuppressive properties (19–21).

A new appreciation of the significance of neutrophils for the host has emerged in light of recent findings on their heterogeneity and plasticity (16, 22), their ability to survive long term, and their ability to shape adaptive arm immune responses (14–16, 23, 24). Neutrophils regulate immune hyper and hypoactivation via a release of inflammatory and toxic mediators and by curbing excessive immune responses (16, 25). The altered functionality of neutrophils can lead to severe inflammatory complications and sepsis (26). Neutrophils colocalize and actively communicate with T cells in draining lymph nodes and other organized lymphoid tissues in which they are involved in negative regulation of T cell function via production of ROS and arginase-1 (15, 27–32). We have recently described a presence of immunosuppressive neutrophils in the blood of HIV-1-infected patients that are likely induced by microbial translocation and suppress T cell function via the production of ROS and programmed death PD-1/PD-L1/interaction (33). Recent studies have identified an immunosuppressive population of CD16⁺CD62L^{low} neutrophils that is induced in human volunteers following injection of a low dose of bacterial LPS and inhibits T cell function by local release of hydrogen peroxide (31) and via PD-L1/PD1 axis.

In sepsis, trauma, and various chronic inflammatory conditions, a population of low-density neutrophils (LDNs) with immunosuppressive properties has been detected (23, 30, 33, 34). In autoimmune diseases, LDNs have been associated with enhanced NETosis and extensive endothelial damage (35). A similar population of granulocytic myeloid-derived suppressor cells (G-MDSCs) has been reported by multiple studies, primarily in patients with cancer (30, 34, 36, 37). Both LDNs and G-MDSCs exert low-density phenotype and cosegregate in the PBMC fraction on a density gradient. It is unclear at present whether LDN and G-MDSC populations are identical or differ in their phenotype, origin, and functional properties (30). Furthermore, it remains to be established whether LDNs/G-MDSCs originate by granulopoiesis from dedicated suppressive progenitors in the bone marrow or, alternatively, they represent a functional subset of neutrophils that is acquired the immunosuppressive phenotype in response to specific signals in the periphery (30). Both LDNs and G-MDSCs display a remarkable ability to suppress T cell-mediated immune responses by multiple mechanisms, including production of ROS, the release of arginase-1 resulting in a depletion of arginine and downregulation of TCR ζ chain, production of regulatory cytokines, and induction of regulatory T cells

(30, 32, 34). LDNs/G-MDSCs are believed to serve as a negative feedback mechanism preventing extensive damage to the host in sepsis and inflammation (32).

The goal of the current study was to determine the phenotype of granulocytes in CVID patients with an emphasis on possible regulatory effect on T cell function. We present evidence that neutrophils in CVID patients acquire a specific activated phenotype and exert potent T cell suppressive activity, a previously unrecognized mechanism of immune suppression in CVID patients.

Materials and Methods

Patients and healthy donors

All participants in the study were white and from South Moravian region of Czech Republic. The study was approved by the Medical Ethics Committee of St Anne's University Hospital, Brno, Czech Republic. Informed consent was obtained from all volunteers prior to the inclusion in the study. A total of 46 CVID patients (25 females, 21 males; median age 45, range 22–82 y) and 44 healthy donors (23 females, 21 males; median age 41, range 19–78 y) were recruited. All patients fulfilled the International Consensus Document diagnostic criteria for CVID (38). Clinical characteristics of the study population are described in Table I. CVID patients were treated with regular i.v. (IVIG) ($n = 25$) or s.c. (SCIG) ($n = 21$) substitution. None of the patients suffered from opportunistic infections typical for late-onset combined immunodeficiency (39). One patient recently had splenectomy for splenomegaly and hypersplenism. One patient underwent partial gastrectomy for gastric cancer; no other malignancies were detected in any of the participants. Three patients were on long-term steroid treatment (owing to granulomatous disease, lung fibrosis, and demyelinating disease). One patient was treated with combined immunosuppressives (steroids and leflunomide) owing to lung fibrosis, arthritis, neurologic involvement, and diarrhea.

Cell isolation

Blood samples for isolation of PBMCs and T cells of patients on IVIG treatment were collected before the IVIG infusion. PBMCs and neutrophils were isolated from the blood harvested in EDTA-containing vacutainers by density gradient centrifugation ($400 \times g$, 30 min) using Ficoll-Paque (Pharmacia, Uppsala, Sweden) and washed twice with PBS supplemented with 5% BSA (Sigma-Aldrich, St. Louis, MO). Following centrifugation, the upper mononuclear cell layer was removed, and the lower granulocyte layer was collected and resuspended. Erythrocytes were lysed using isotonic NH_4Cl erythrocyte lysis buffer (170 mM NH_4Cl , 10 mM KHCO_3 , 20 mM EDTA, pH 7.3) at room temperature. Cells were cultured in RPMI 1640 (Sigma-Aldrich) supplemented with 10% heat-inactivated FBS (HyClone, South Logan, UT), 100 U/ml penicillin, 100 mg/ml streptomycin, and 2 mM L-glutamine (HyClone), further referred to as complete RPMI medium. T cells were isolated from peripheral blood using RoboSep Human CD3 Positive Selection Whole Blood kit (STEMCELL Technologies, Rockford, IL). Separation was performed on the instrument RoboSep-S (STEMCELL Technologies) according to the manufacturer's instructions.

ELISA for the detection of neutrophil activation markers and cytokines

To prevent neutrophil degranulation and release of enzymes, EDTA blood was collected on ice. Within 20 min after the blood draw, the plasma was separated by centrifugation ($1500 \times g$, 4°C, 15 min). Plasma was removed and transferred to fresh polypropylene tube without disturbing white cells in the buffy coat. Harvested plasma was centrifuged second time under the same conditions to separate any remaining WBCs. Samples were cryopreserved at -80°C . ELISA assays for the determination of neutrophil gelatinase-associated lipocalin (NGAL; Hycult Biotech, Plymouth Meeting) and IFN- γ (BioLegend, San Diego, CA) were performed according to the manufacturers' protocols.

Cell culture

PBMCs and T cells were stimulated with 1 $\mu\text{g}/\text{ml}$ purified plate-bound anti-CD3 mAb (CD3 mAb; clone Hit-3a; BioLegend) and with added 0.3 $\mu\text{g}/\text{ml}$ anti-CD28 mAb (clone CD28.2; eBioscience) for 18 h in complete RPMI medium in 96-well flat-bottom plates with a starting concentration of 2×10^5 cells per well, (1×10^6 per ml) of PBMCs or 10^5 cells per well (1×10^6 ml) of T cells. For detection of cytokines by intracellular staining, Brefeldin A (10 $\mu\text{g}/\text{ml}$; Sigma-Aldrich) was added for the last 4 h. Cell

proliferation was determined by the incorporation of thymidine analog BrdU (PerkinElmer, Waltham, MA) into newly synthesized DNA and detection with anti-BrdU Ab. For proliferation, PBMCs and T cells were stimulated with 1 $\mu\text{g}/\text{ml}$ purified plate-bound anti-CD3 mAb and added to 0.3 $\mu\text{g}/\text{ml}$ anti-CD28 mAb for 48 h in complete RPMI medium at a starting concentration of 2×10^5 cells per well (1×10^6 per ml) for PBMCs and 1×10^5 cells per well for T cells (1×10^6 per ml) in 96 flat-bottom cells. BrdU was added for the last 12 h. Proliferating cells were processed using the DELFIA Cell proliferation kit (PerkinElmer) following the manufacturer's protocol. Briefly, cells are incubated with the nonradioactive pyrimidine analog BrdU to allow its incorporation into newly synthesized DNA. Subsequently, europium-labeled anti-BrdU Abs are used to detect the level of BrdU incorporation via time-resolved fluorescence, a measurement of the Eu-fluorescence in a time-resolved fluorometer EnSight (PerkinElmer). For the neutrophil/T cell suppression assays, purified T cells or PBMCs were stimulated with plate-bound anti-CD3 (1 $\mu\text{g}/\text{ml}$) and soluble anti-CD28 (0.3 $\mu\text{g}/\text{ml}$) Abs for 18 h for production of cytokines and 48 h for proliferation test. Neutrophils were cocultured with CD3⁺ T cells or PBMCs at 1:3 T cell/neutrophil ratio (10^5 cells; 3×10^5 neutrophils per well). To address the mechanism of neutrophil-mediated suppression of T cells, catalase (CAT; 1000 U/ml) and superoxide dismutase (SOD; 200U/ml; Sigma-Aldrich) were added to media to neutralize ROS, *N*^G-hydroxy-L-arginine monoacetate (L-NHA; 2.5 $\mu\text{g}/\text{ml}$) was added to inhibit arginase-1, and *N*^ω-monomethyl-L-arginine acetate salt (L-NMMA; 2.5 $\mu\text{g}/\text{ml}$; Sigma-Aldrich) was added to inhibit the function of inducible NO synthase (iNOS). Anti-PD-L1 (clone 29E.2A3) (5 $\mu\text{g}/\text{ml}$) and anti-PD-1 (clone EH12.2H7) (5 $\mu\text{g}/\text{ml}$, BioLegend) Abs were added to inhibit PD-L1/PD-1 signaling pathway.

Intracellular cytokine staining

Cells were washed, fixed, permeabilized using Intracellular Fixation and Permeabilization Buffer Set (eBioscience, San Diego, CA), and stained with IFN- γ -BV421 (clone 4S.B3) (BioLegend). Dead cell exclusion was performed using aqua-fluorescent reactive dye LIVE/DEAD Fixable Stain Kit (Invitrogen, CA). T cell staining was performed using CD4-PE-Cy7 (clone SF112T4D11), CD8-allophycocyanin A750 (clone B9.11) (Beckman Coulter, Miami, FL), CD3-allophycocyanin (clone SK7) (BD Biosciences, San Jose, CA), and CD25-PerCP-Cy5.5 (clone BC96) (BioLegend). Gating strategy for the analysis of the expression of CD25 and intracellular production of INF- γ is depicted in Supplemental Fig. 1.

Flow cytometry characterization of neutrophils and LDNs

For the determination of activation markers on the surface of neutrophils, mAbs were used in the following combinations: 1) CD15-FITC (clone HI98), CD80-PE (clone 2D10), CD14-PerCP-Cy5.5 (clone M5E2), CD274-allophycocyanin (PD-L1) (clone 29E.2A3), CD62L-BV421 (clone DREG-56) (BioLegend) and CD16-allophycocyanin A750 (clone 3G8), CD45-Krome Orange (clone J33) (Beckman Coulter); 2) CD15-FITC, CD87-PE (clone VIM5), CD14-PerCP-Cy5.5, CD11a-PE-Cy7 (clone HI111), HLA-DR-BV421 (clone L243), CD11b-BV 510 (clone ICRF44), (BioLegend), and CD45-allophycocyanin-H700 (clone 2D1) (BD Biosciences); 3) CD15-FITC, CCR3-PE (clone 5E8), CD14-PerCP-Cy5.5, CD64 PC7 (clone 10.1) CXCR4-allophycocyanin (clone 12G5), CD62L-BV421, CD11b-BV 510, CD16-allophycocyanin A750; 4) CD15-FITC, CCR3-PE, CD14-PerCP-Cy5.5, CD64 PE-Cy7, CD54-allophycocyanin (clone HA58), CD62L-BV421, CD11b-BV 510, CD16-allophycocyanin A750; 5) CD15-FITC, CCR3-PE, CD14-PerCP-Cy5.5, CD10-allophycocyanin (clone HI10a), CD62L-BV421, CD11b-BV 510, and CD16-allophycocyanin A750. Briefly, fresh blood samples were incubated for 30 min at 4°C in the dark with mAbs. The erythrocytes were lysed by Multi-Q-Prep Lysing Workstation (Beckman Coulter). Samples were acquired using a Navios flow cytometer (10 colors, three lasers; Beckman Coulter), and cytometry data (LMD files) were analyzed using Kaluza software (Beckman Coulter). The data are presented as the median fluorescence intensity for each cell subset. Gating strategy for the analysis of neutrophils is depicted in Supplemental Fig. 2A.

For the characterization of LDNs, freshly isolated PBMCs were incubated for 30 min in the dark with the following mAbs: CD15-FITC, CCR3-PE, CD14-PerCP-Cy5.5, CD33-PE-Cy7 (clone D3HL60.251), CD10-allophycocyanin or CXCR4-allophycocyanin or CD54-allophycocyanin, CD62L-BV510 (BioLegend), CD16 allophycocyanin A750, and CD45-Krome Orange (Beckman Coulter). Gating strategy for the analysis of LDNs is depicted in Supplemental Fig. 2B.

Ex vivo stimulation of blood with bacterial products

Whole blood freshly obtained from healthy donors was either not stimulated or stimulated with fMLF (10 μM ; Sigma-Aldrich) or LPS (1 $\mu\text{g}/\text{ml}$,

Escherichia coli 0111:B4; Sigma-Aldrich) at 37°C for the indicated time and immediately stained with CD14-allophycocyanin/Fire750 (clone 63D3), CD274-PE-Cy7 (PD-L1; 29E.2A3), CD11b-PerCP-Cy5.5 (ICRF44; BioLegend), CD62L-BV711 (DREG-56), CD193-BV510 (CCR3; 5E8; BD Biosciences), CD15-eFluor450 (HI98), and CD16-allophycocyanin (eBioCB16; eBioscience) for 30 min at 4°C. Samples were washed with cold wash Dulbecco's PBS buffer with EDTA (1 mM EDTA in DPBS) and centrifuged at $200 \times g$ for 5 min to remove unbound Abs. Samples were lysed with 1 ml of 1-step Fix/lyse buffer (Invitrogen/Thermo Fisher Scientific) in the dark at room temperature for 15 min, washed, and resuspended in equal parts of 2% FBS in DPBS and intracellular Fixation buffer (Thermo Fisher Scientific) prior to the analysis on the Attune NxT flow cytometer (Thermo Fisher Scientific). Cytometry data were analyzed by FlowJo (FlowJo, Ashland, OR). For the analysis of induction of LDNs in whole blood ex vivo, whole blood from healthy donors was either not stimulated or stimulated with LPS (1 $\mu\text{g}/\text{ml}$) or fMLF (10 μM) at 37°C for the indicated time; PBMCs were purified by gradient centrifugation, and LDNs were characterized as described above.

Statistics

Intergroup differences were analyzed using the nonparametric Mann-Whitney *U* test or Wilcoxon signed-rank test as appropriate. Correlations were assessed using the Spearman rank correlation test. Fisher exact test was used for the analysis of categorical data. The *p* values <0.05 (two-tailed) were considered statistically significant. Data were analyzed using GraphPad Prism 5 (GraphPad Software, CA).

Results

CVID patients display elevated levels of NGAL in plasma

Granulocytes have been previously shown to contribute to several autoimmune and inflammatory complications in CVID patients, including granuloma formation and chronic lung, intestinal, and other organ inflammation (38). We have previously reported that CVID patients display increased levels of myeloid cell-derived cytokines and chemokines in plasma, including factors involved in granulopoiesis and neutrophil activation (10). To further address the potential role of granulocytes in CVID pathogenesis, we analyzed immune cell populations and plasma markers of granulocytic activation in 46 CVID patients and 44 healthy donors (clinical parameters of the study population are described in Table I). CVID patients displayed increased absolute number of neutrophils compared with controls (3.45×10^9 per l versus 2.71×10^9 per l; *p* = 0.014; Mann-Whitney *U* test) (Fig. 1) whereas the absolute number of lymphocytes was decreased (1.43×10^9 per l versus 1.97×10^9 per l; *p* < 0.0001), consistent with a previous study (5). Interestingly, the plasma concentration of NGAL, a marker of neutrophil activation and degranulation, was significantly increased in CVID patients compared with healthy controls (*p* < 0.0001; Mann-Whitney *U* test) (Fig. 2). Because the elevated plasma level of NGAL could be caused by the increase in the absolute number of circulating neutrophils, normalization to absolute neutrophil count was performed. Following normalization, the statistical significance of intergroup differences was preserved (*p* < 0.0001) (Fig. 2). The intergroup differences remained significant after exclusion of CVID patients with C-reactive protein (CRP) >10 mg/l (*n* = 7; *p* < 0.0001), indicating that the increase in neutrophil activation and degranulation marker could not be attributed solely to the level of systemic immune activation. No correlations between the concentration of NGAL and other laboratory and clinical parameters were observed. No statistically significant difference in plasma levels of arginase-1 between CVID patients and healthy donors was observed (Supplemental Fig. 3).

Neutrophils from CVID patients exhibit an activated phenotype

To further address the potential role of granulocytes in CVID pathogenesis, we evaluated the levels of neutrophil surface markers of activation and potential suppressor activity in fresh blood of

Table I. Clinical characteristics of the study population

	IVIG (n = 27)	SCIG (n = 19)	Total (n = 46)
F/M	14/13	11/8	25/21
Age, mean (range)	43.5 (23–77)	46.9 (21–83)	45.5 (21–83)
Length of Ig treatment, mean (range)	11.52 (0.17–25)	9.89 (1–21)	10.85 (0.17–25)
Bronchiectasis, n (%)	14/25 ^a (56)	3/19 (16)	17/44 ^a (39)
Autoimmune diseases, n (%)	4/27 (15)	7/19 (37)	11/46 (24)
Granuloma, n (%)	4/25 ^a (16)	3/19 (16)	7/44 ^a (16)
Chronic diarrhea, n (%)	4/27 (15)	5/19 (26)	9/46 (20)

^aData concerning bronchiectasis and granulomas were not available in two patients.
F, female; M, male.

CVID patients and healthy donors. Whole blood neutrophils were gated as side light scatter (SSC)^{high} CD45⁺ CD15⁺ population, and the surface levels of CD11a, CD11b, CD16, CD62L, CD80, CD87, PD-L1, and HLA-DR were examined. A significant increase of median fluorescence intensity of CD11b ($p < 0.01$) and PD-L1 ($p < 0.002$), and decreases of CD16 ($p < 0.01$), CD62L ($p < 0.0005$), and CD80 ($p = 0.0002$, Mann–Whitney U tests) were observed on neutrophils from CVID patients compared with neutrophils from healthy donors (Fig. 3). CD11a, CD87, HLA-DR, CD10, CXCR4, and CD54 levels were not significantly different between the experimental groups. Surface levels of CD10 and CXCR4 are depicted in Supplemental Fig. 4. Phenotypic analysis of T cells of CVID patients revealed an increased expression of PD-1 on both CD4⁺ and CD8⁺ T cells compared with controls, consistent with previous reports (9, 10). However, no significant correlations were found between the levels of PD-L1 on neutrophils and PD-1 on T cells in CVID patients ($p = 0.2$ and $p = 0.4$ for PD-1 on CD4⁺ and CD8⁺ T cells, respectively; Spearman correlation test).

Neutrophils from CVID patients suppress T cell activation and production of IFN- γ

CD11b⁺CD16⁺CD62L^{dim} neutrophils were previously described as a unique circulating population mediating the suppression of T cell activation and cytokine production (31, 32). We have, therefore, assessed the ability of neutrophils from CVID patients to suppress the T cell activation upon CD3/CD28 stimulation *ex vivo*. Surface CD25 expression was higher on CD8⁺ T cells of CVID patients compared with controls ($p < 0.02$) but was significantly reduced on

T cells following cocultivation with autologous neutrophils ($p = 0.003$; Wilcoxon test) (Fig. 4A). In contrast, neutrophils suppressed CD4⁺ T cell activation in healthy controls ($p = 0.01$) but not CVID patients ($p = 0.1$) (Fig. 4B). Intracellular production of IFN- γ by CD8⁺ T cells following CD3/CD28 stimulation in the absence of neutrophils was higher in CVID patients ($p < 0.0001$) (Fig. 4C) and correlated with the frequency of effector memory CCR7[−]CD45RO⁺ CD8⁺ T cells in CVID patients ($r = 0.4$; $p = 0.003$), but not in healthy donors ($r = 0.3$; $p = 0.09$; Spearman test). Importantly, the production of IFN- γ by CD8⁺ T cells of CVID patients upon CD3/CD28 stimulation was suppressed following cocultivation with autologous neutrophils ($p = 0.005$); however, no effect was observed in healthy donors ($p = 0.6$; Wilcoxon test). Intracellular production of IFN- γ by CD4⁺ T cells following CD3/CD28 stimulation in the absence of neutrophils was higher in CVID patients ($p = 0.004$) (Fig. 4D) and correlated with the frequency of effector memory CCR7[−]CD45RO⁺ CD4⁺ T cells in CVID patients ($r = 0.3$; $p = 0.03$), but not in healthy donors ($r = 0.2$; $p = 0.27$; Spearman test). No significant difference was found in the production of IFN- γ in CD4⁺ T cells after coculture with neutrophils of CVID patients or healthy controls. IFN- γ protein accumulation in the medium upon CD3/CD28 stimulation was lower in cocultures of T cells with neutrophils from CVID patients ($p = 0.02$) as well as healthy controls ($p = 0.04$; Wilcoxon test) (Fig. 4E). The production of IFN- γ in the medium upon CD3/CD28 stimulation was higher in the culture of T cells in CVID patients $p < 0.005$; Mann–Whitney U test). Suppressive activity of CVID neutrophils was not significantly associated with clinical symptoms, including bronchiectasis, splenomegaly, chronic diarrhea, granuloma, or autoimmunity (tested using Fischer exact test), duration of Ig treatment, or the time from the first manifestation of ID symptoms (tested using Mann–Whitney U test).

Neutrophil-mediated immune suppression of IFN- γ production by activated T cells in CVID patients is dependent on ROS

To address the mechanisms of neutrophil-mediated suppression of T cell function, T cells were cocultured with neutrophils in media supplemented with CAT and SOD to neutralize ROS, iNOS inhibitor L-NMMA, arginase inhibitor L-NHA, or anti-PD-L1 and anti-PD-1 Abs to inhibit the PD-L1/PD1 pathway. The production of IFN- γ by CD3⁺CD8⁺ T cells following stimulation with CD3/CD28 in coculture with neutrophils from CVID patients was restored in the presence of CAT and SOD (Fig. 5A). Inhibition of PD-L1/PD-1 signaling resulted in partial restoration of neutrophil-mediated suppression of the production of IFN- γ by CD3⁺CD8⁺ T cells in CVID patients (Fig. 5A). In healthy donors, the production of IFN- γ by stimulated CD3⁺CD8⁺ T cells cocultured with neutrophils was restored only in the presence of ROS inhibitors ($p < 0.0001$; Wilcoxon test). No significant alteration of the production of IFN- γ by CD4⁺ T cells stimulated in the presence of inhibitors was observed in CVID patients or healthy controls. Full restoration of neutrophil-mediated suppression of extracellular

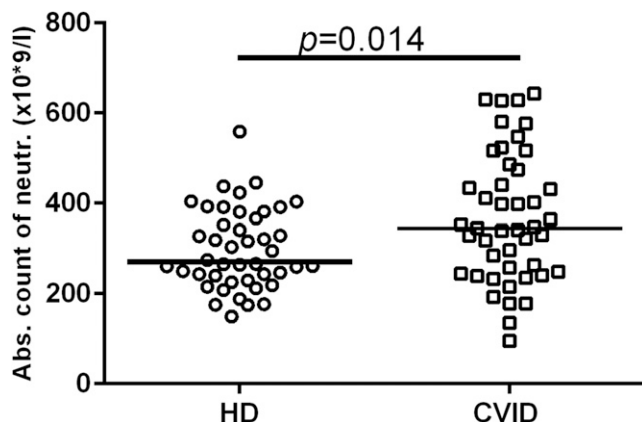
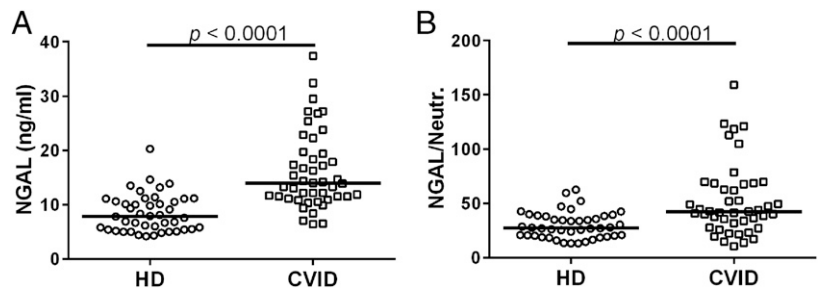


FIGURE 1. CVID patients display increased absolute neutrophil blood count. Total leukocyte counts were determined in whole blood. The neutrophils were gated as CD45⁺CD15⁺ CD16⁺SSC^{high} cells. The absolute number of circulating neutrophils was determined based on the flow cytometry analysis of population frequency and absolute leukocyte count. Horizontal bars represent medians; data were analyzed using the Mann–Whitney U test (CVID: $n = 46$; HD: $n = 44$). HD, healthy donors.

FIGURE 2. CVID patients display elevated plasma levels of NGAL. Plasma NGAL concentrations were determined using ELISA. The absolute concentration of NGAL (**A**) and concentration of NGAL normalized to absolute neutrophil count (**B**) are depicted. Horizontal bars represent medians; data were analyzed using the Mann–Whitney *U* test (CVID: *n* = 46; HD: *n* = 44). HD, healthy donors.



production of IFN- γ by stimulated T cells was observed in the presence of ROS inhibitors in CVID patients (Fig. 5B) as well as in healthy donors ($p < 0.0001$; tested by Wilcoxon test). A partial restoration was observed in the presence of the inhibitor of arginase-1 or blockade of the PD-L1/PD-1 pathway in CVID patients (Fig. 5B) as well as in healthy donors ($p = 0.0002$ for both L-NHA and PD-L1/PD-L1 inhibition; tested by Wilcoxon test).

Neutrophils from CVID patients suppress the proliferation of autologous T cells

To evaluate the suppressive effect of CVID neutrophils on autologous T cells, T cells were stimulated with CD3/CD28 in the presence or absence of neutrophils and proliferation was analyzed

after 48 h. The proliferation of T cells was significantly reduced following incubation with autologous neutrophils from CVID patients ($p = 0.03$; Wilcoxon test) (Fig. 6A). No significant effect was detected following coculture of T cells of healthy donors with autologous neutrophils (Fig. 6A). To address the mechanism underlying neutrophil-mediated suppression of T cell proliferation in CVID patients, the experiments were performed in the presence of inhibitors of ROS, iNOS, arginase-1, and PD-L1/PD1 pathway. No statistically significant effect of inhibitors of any of the regulatory pathways was observed (Fig. 6B). Therefore, the mechanism of neutrophil-mediated inhibition of T cell proliferation in CVID patients remains unclear. Importantly, a negative correlation was observed between the expression of CD62L on fresh blood

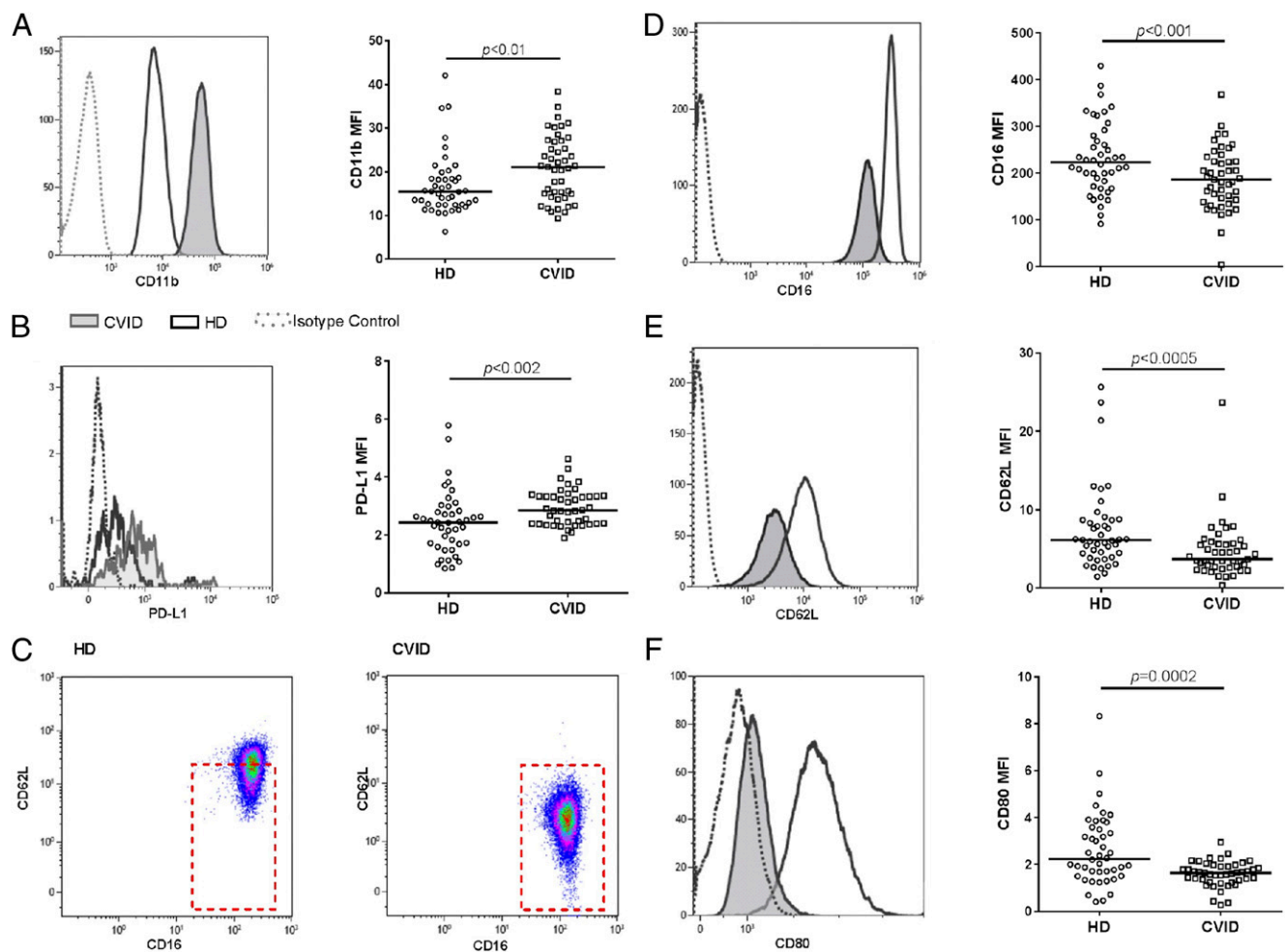
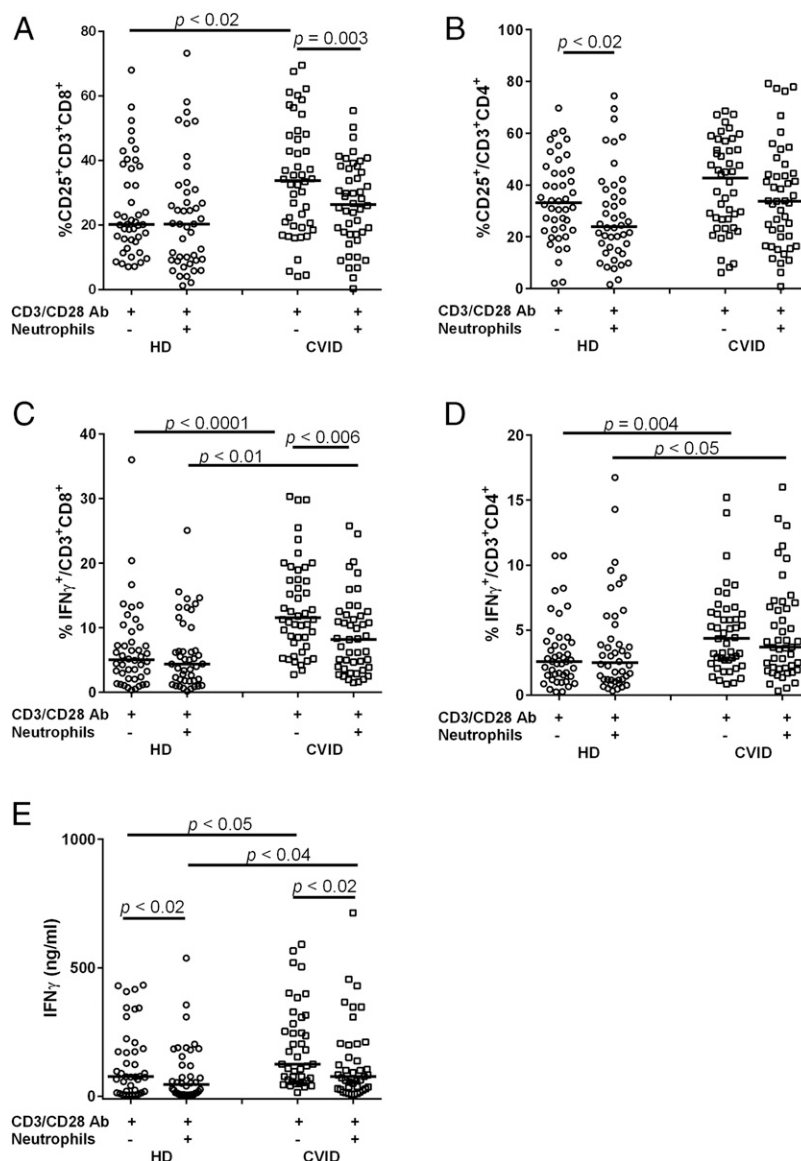


FIGURE 3. Neutrophils from CVID patients exhibit an activated phenotype. Neutrophils were gated as CD45⁺CD15⁺CD16⁺SSC^{high} cells. (**A** and **B**) Increased expression of CD11b (**A**) and PD-L1 (**B**) on neutrophils in fresh blood of CVID patients. (**C**) Decreased levels of CD16 and CD62L on neutrophils in fresh blood of CVID patients; representative examples. (**D**–**F**) Decreased expression of CD16 (**D**), CD62L (**E**), and CD80 (**F**) on neutrophils in fresh blood of CVID patients; cumulative data. Horizontal bars represent medians; data were analyzed using the Mann–Whitney *U* test (CVID: *n* = 46; HD: *n* = 44). HD, healthy donors.

FIGURE 4. Neutrophils from CVID patients suppress T cell activation and production of IFN- γ . Purified CD3 $^{+}$ T cells were isolated from healthy donors and CVID patients and stimulated with anti-CD3 (1 μ g/ml) and anti-CD28 (0.3 μ g/ml) Abs in the absence or presence of autologous neutrophils at 1:3 T cell/neutrophil ratio (1×10^5 T cells; 3×10^5 neutrophils per well). After 18 h of coculture, the frequencies of CD25 $^{+}$ and IFN- γ^{+} CD4 $^{+}$ and CD8 $^{+}$ T cells were determined by flow cytometry. IFN- γ was determined by intracellular staining. (**A** and **B**) Percentages of CD25 $^{+}$ T cells of total CD3 $^{+}$ CD8 $^{+}$ or CD3 $^{+}$ CD4 $^{+}$ T cells. (**C** and **D**) Percentages of IFN- γ^{+} T cells of total CD3 $^{+}$ CD8 $^{+}$ or CD3 $^{+}$ CD4 $^{+}$ T cells. (**E**) Coincubation of T cells with autologous neutrophils in culture supernatants in response to the stimulation with CD3/CD28. Horizontal bars represent medians, which were analyzed using Wilcoxon or Mann-Whitney U test as appropriate (CVID: $n = 46$; HD: $n = 44$). HD, healthy donors.



neutrophils and their capacity to suppress autologous T cell proliferation *ex vivo* ($r = -0.5$; $p = 0.002$; Spearman test) (Fig. 6C), consistent with the reported suppressive activity of CD62L $^{\text{dim}}$ neutrophils (31, 32). In contrast, no significant correlation was observed in healthy donors (Fig. 6C).

CVID patients display an increased frequency of LDNs/G-MDSCs

LDNs and G-MDSCs have been previously described as specific populations of suppressive granulocytes in cancer, trauma, and other inflammatory conditions (33, 34). Although it remains to be determined whether LDNs and G-MDSCs represent an identical cell population, they have been shown to share many key properties, most notably the low-density phenotype resulting in their retention in the PBMC layer on density gradients. We have addressed whether the frequency LDNs/G-MDSCs, characterized as SSC $^{\text{high}}$ CD33 $^{+}$ CD14 $^{-}$ CD15 $^{+}$ cells in fresh PBMCs, is increased in the blood of CVID patients. As shown in Fig. 7A and 7B, CVID patients exhibited a significantly increased frequency of LDNs in PBMCs compared with healthy donors ($p = 0.02$). A positive correlation was observed between CD11b expression on neutrophils from fresh blood and the frequency of LDNs in CVID patients ($r = 0.4$; $p = 0.007$) and

healthy donors ($r = 0.3$; $p = 0.04$; Spearman test). Next, we examined whether the presence of LDNs is associated with reduced production of IFN- γ by CD3/CD28-activated T cells *ex vivo*. A negative correlation was observed between the frequency of LDNs in PBMCs and intracellular production of IFN- γ by CD8 $^{+}$ T cells in PBMCs of CVID patients ($r = -0.4$; $p = 0.007$) but not healthy donors ($r = -0.05$; $p = 0.8$; Spearman test). CD10, CXCR4, and CD54 levels were not significantly different on LDNs between the experimental groups. No statistically significant correlation between the frequency of LDNs and administration of IVIG or any other laboratory and clinical parameters was observed.

Ex vivo stimulation of blood with bacterial products reduces neutrophil surface levels of CD62L, increases CD11b, and induces LDNs

Others and we have previously described evidence of microbial translocation in CVID patients (10–12). Circulating products of microbial translocation may be responsible for the activated neutrophil phenotype and altered profile of myeloid cell-derived cytokines and chemokines in CVID patients (10, 11). To address this possibility, fresh blood of healthy donors was stimulated with bacterial products fMLF and LPS. As shown in Fig. 8, stimulation

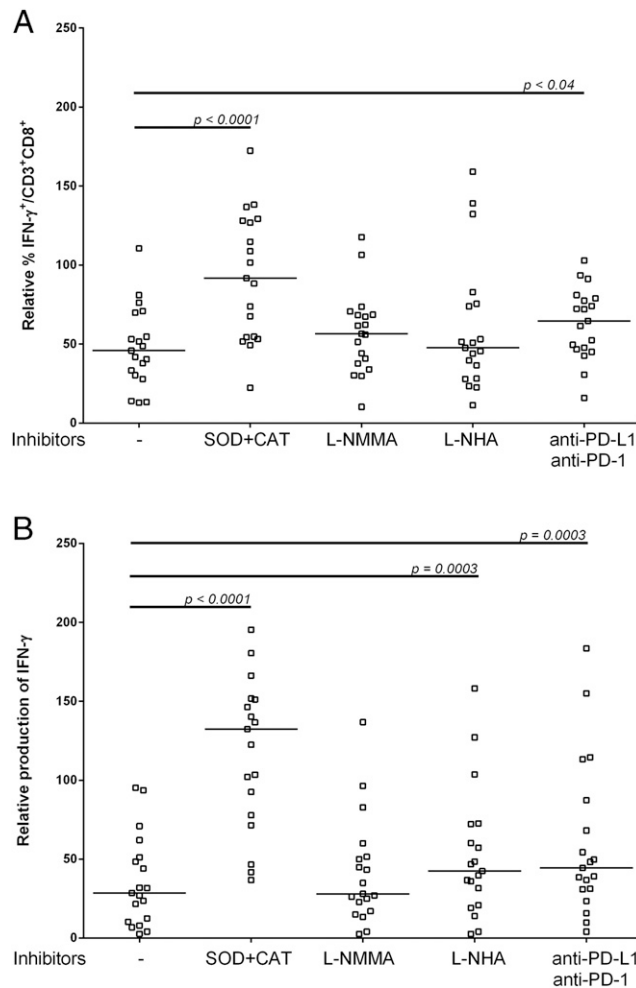


FIGURE 5. Mechanisms of neutrophil-mediated suppression of IFN- γ production by activated T cells in CVID patients. Purified CD3⁺ T cells were isolated from CVID patients and stimulated with anti-CD3 (1 μ g/ml) and anti-CD28 (0.3 μ g/ml) Abs in the presence of autologous neutrophils (10^5 T cells; 3×10^5 neutrophils per well) in the presence or absence SOD (200 U/ml) and CAT (1000 U/ml), L-NMMA (2.5 μ g/ml), L-NHA (2.5 μ g/ml), or anti-PD-1 (5 μ g/ml) and anti-PD-L1 (5 μ g/ml) Abs. After 18 h of coculture, the relative frequency of IFN- γ ⁺ of CD3⁺CD8⁺ cells compared with T cells stimulated in the absence of neutrophils is depicted (**A**). (**B**) IFN- γ concentration was determined in culture supernatants from cell cultures described in (**A**). Relative production of IFN- γ compared with T cells stimulated in the absence of neutrophils is depicted. Analyzed using Wilcoxon test (CVID: $n = 19$).

with LPS and fMLF lead to a rapid increase of surface levels of a degranulation marker CD11b and a decrease in the levels of CD62L. In contrast, the levels of CD16 were not significantly affected by either stimulation. The surface level of suppressor molecule PD-L1 was increased; however, the change did not reach statistical significance. Importantly, stimulation of whole blood from healthy donors ($n = 4$) with bacterial products fMLF or LPS increased the frequency of LDNs in the PBMC layer following density gradient centrifugation by 27-fold ($p = 0.02$) and 18-fold ($p = 0.02$), respectively (Fig. 9).

Discussion

In this study, we show that neutrophils from CVID patients exhibit significantly altered phenotype characterized by reduced surface levels of CD16, CD62L, and CD80 and elevated levels of CD11b and PD-L1. In addition, the presented data indicate that CVID

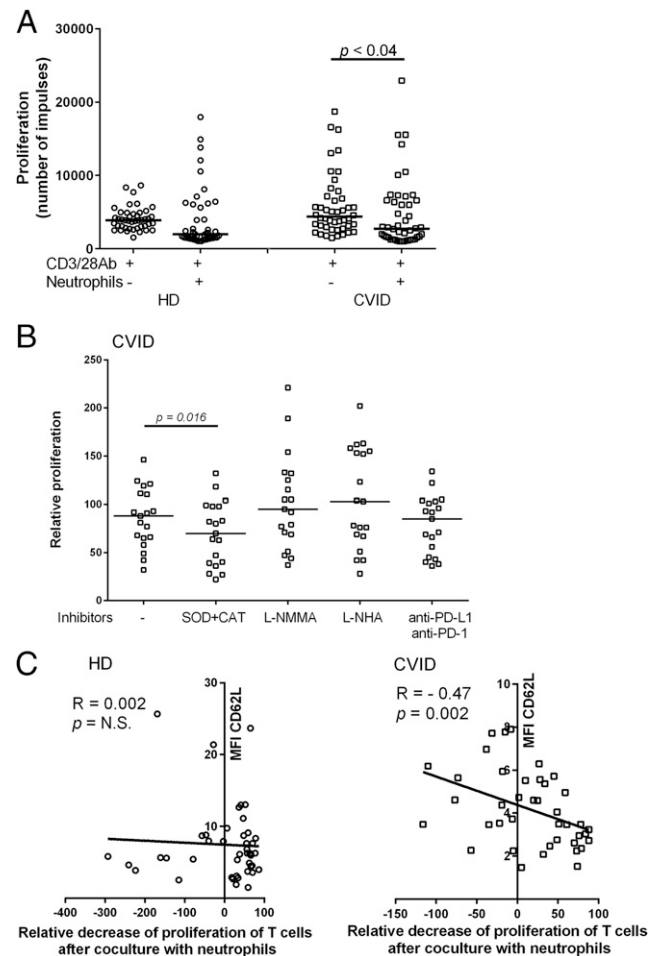


FIGURE 6. CVID neutrophils suppress the proliferation of autologous T cells. (**A**) Purified CD3⁺ T cells from healthy donors and CVID patients were stimulated with anti-CD3 (1 μ g/ml) and anti-CD28 (0.3 μ g/ml) Abs in the absence or presence of autologous neutrophils at 1:3 T cell/neutrophil ratio (1×10^5 T cells; 3×10^5 neutrophils per well). After 48 h of coculture, cell proliferation was determined by the incorporation of BrdU into newly synthesized DNA. Analyzed using the Mann-Whitney U test (CVID: $n = 46$; HD: $n = 44$). (**B**) Mechanism of neutrophil-mediated suppression of T cell proliferation. Purified CD3⁺ T cells were isolated from CVID patients and stimulated with anti-CD3 (1 μ g/ml) and anti-CD28 (0.3 μ g/ml) Abs in the presence of autologous neutrophils and in the presence or absence SOD (200 U/ml) and CAT (1000 U/ml), L-NMMA (2.5 μ g/ml), L-NHA (2.5 μ g/ml), or anti-PD-1 (5 μ g/ml) and anti-PD-L1 (5 μ g/ml) Abs. After 48 h of coculture, cell proliferation was determined by the incorporation of BrdU. Relative proliferation compared with T cells stimulated in the absence of neutrophils is depicted. Analyzed using Wilcoxon test (CVID: $n = 19$). (**C**) Correlation between the level of CD62L on fresh blood neutrophils and the relative decrease of T cell proliferation following incubation with autologous neutrophils from healthy donors and CVID patients. Analyzed using Spearman rank correlation test; r and p values are indicated; lines represent linear regression analysis (CVID: $n = 46$; HD: $n = 44$). HD, healthy donors.

neutrophils actively suppress the activation and IFN- γ production by CD8⁺ T cells via the production of ROS and partially via PD-L1/PD-1 regulatory pathway. This observation may be of high potential importance as it provides a qualitatively new view on the mechanisms of immune suppression in CVID and potentially other immunodeficiencies and inflammatory conditions.

The mechanisms causing altered neutrophil phenotype in CVID are unclear. It is tempting to speculate that changes in neutrophil

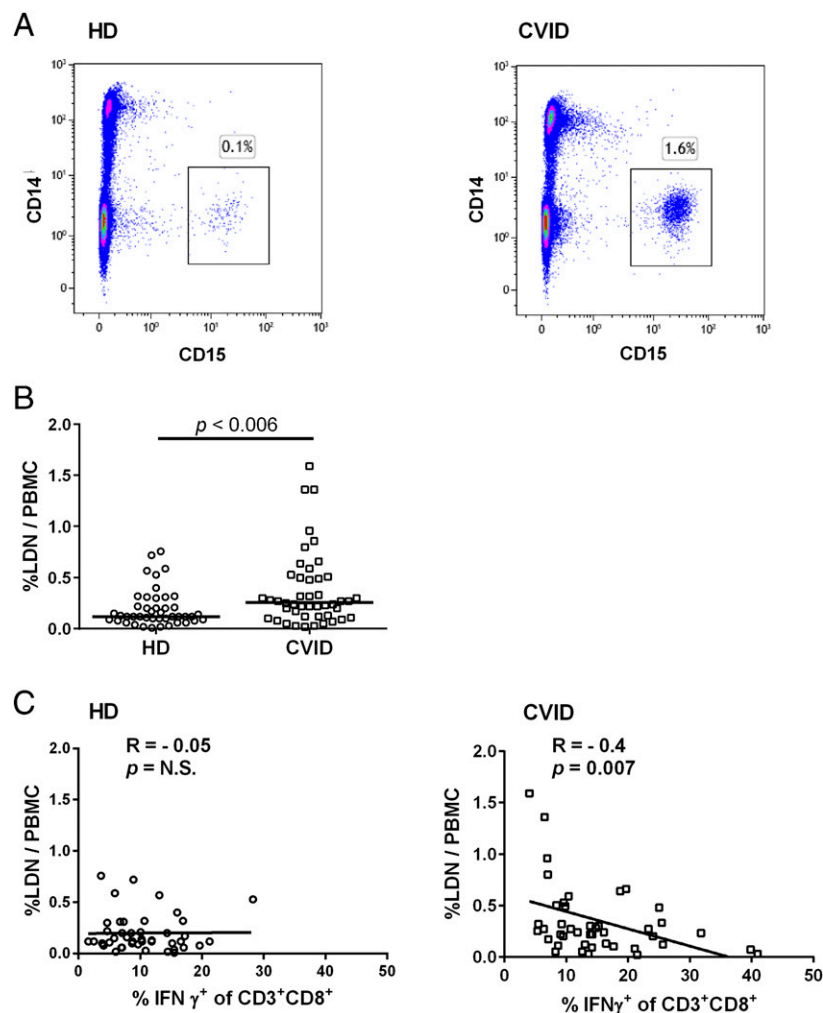


FIGURE 7. The frequency of LDNs is increased in the blood of CVID patients. LDNs were detected as CD45⁺CD15⁺CCR3⁻CD16⁺ cells in the PBMC fraction following density gradient centrifugation. **(A)** Representative flow cytometry plots of LDNs detected in PBMCs obtained from a healthy donor and CVID patient. **(B)** Cumulative frequencies of LDNs in PBMCs of healthy donors and CVID patients. Analyzed using the Mann–Whitney U test. **(C)** Correlation between the frequency of LDNs and the percentage of IFN- γ ⁺ CD3⁺CD8⁺ T cells following ex vivo stimulation with CD3/CD28. Analyzed using the Spearman rank correlation test; lines represent linear regression (CVID: $n = 46$; HD: $n = 44$). HD, healthy donors.

population are driven by chronic microbial translocation, a process of transfer of whole bacteria and microbial products from the intestinal lumen into the systemic circulation. Low level of microbial translocation occurs in healthy individuals; however, its extent dramatically increases in various pathological conditions including inflammatory bowel disease, celiac disease, visceral leishmaniasis, dengue virus infection, HIV infection, hepatic cirrhosis caused by alcohol abuse, or hepatitis B and C infections (40, 41). Translocation of bacterial and fungal products results in activation of both innate and acquired immune response mechanisms (10). Others and we have previously presented evidence of chronic microbial translocation in CVID patients (10–13, 42). Complex interactions between LPS, CD14, and TLR 4 results in the secretion of soluble CD14 (sCD14) from myeloid cells. Serum levels of sCD14 represent a marker of bacterial translocation and endotoxemia (43–45). We have previously demonstrated that CVID patients display elevated concentration of plasma sCD14 and other factors consistent with microbial translocation (10). One study showed that, in addition to elevated sCD14, CVID patients display chronic monocytic activation (12). Other investigators showed increased LPS levels together with increased sCD25 in CVID patients (13). We demonstrated that CVID patients display an altered profile of cytokine production, namely reduced serum levels of cytokines produced by CD4⁺ Th1 cells (IFN- γ , IL-2), Th2 (IL-9, IL-13), and Th17 (IL-17). In contrast, CVID is associated with elevated serum levels of G-CSF, CXCL-10/IP-10, IL-1R antagonist, TNF- α , IL-10, IL-12 (p40), CCL-2/MCP-1,

and eotaxin (10). This cytokine signature is consistent with an ongoing activation of cells of monocytic and granulocytic lineages. The concentration of G-CSF, a key granulopoietic regulator and a central mediator of emergency granulopoiesis (18), was increased by over 2-fold in CVID patients compared with healthy donors ($p = 0.0001$) (10).

Emergency granulopoiesis is a process of rapid generation of neutrophils via increased myeloid progenitor cell proliferation in the bone marrow in response to systemically disseminated bacterial products or invading pathogens. Pathogen sensing occurs mainly in nonhematopoietic cells through TLR signaling. However, sensing by hematopoietic stem and progenitor cells have also been suggested and might contribute to the overall granulopoietic response (17, 18). Recent studies showed that emergency granulopoiesis is driven by G-CSF produced by endothelial cells in response to LPS signaling via the TLR4/MyD88 pathway (18–20, 46). G-CSF-induced neutrophils undergo an alternative differentiation pathway from common myeloid progenitor and granulocyte/macrophage progenitors, produce ROS, and display potent immunosuppressive properties (19–21). In this study, we observed a 30% increase in the absolute numbers of neutrophils in CVID patients ($p = 0.014$; Fig. 1), consistent with enhanced granulopoiesis. However, the rate of granulopoiesis cannot be easily determined from absolute cell counts due to the contribution of complex processes of cell recruitment, trafficking, survival, and removal (47).

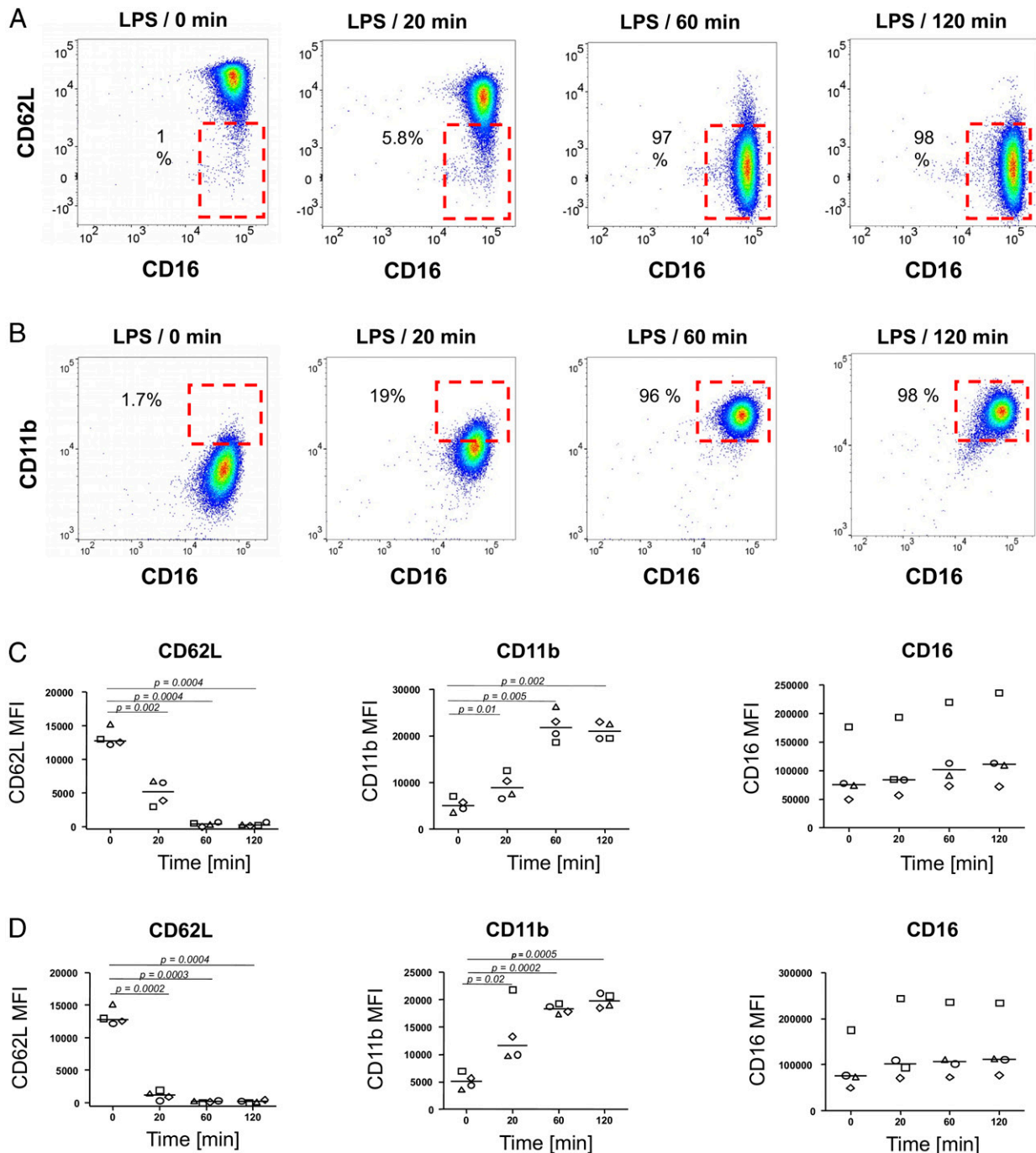


FIGURE 8. Stimulation of whole blood with bacterial products results in a rapid reduction of the neutrophil surface levels of CD62L and increased levels of CD11b. Whole blood from healthy donors was stimulated with bacterial LPS (1 $\mu\text{g}/\text{ml}$) and fMLF (10 μM) for the indicated time. The levels of surface markers were analyzed on SSC^{high} CCR3^{low} CD14^{low} $\text{CD15}^{\text{high}}$ cells. (**A** and **B**) Stimulation of blood with LPS results in a rapid decrease of levels of CD62L and an increase of surface levels of CD11b on neutrophils. (**C** and **D**) Cumulative data depicting the changes in surface marker expression on neutrophils following the stimulation of whole blood with LPS (**C**) or fMLF (**D**). Data obtained from four independent healthy donors and analyzed using Mann–Whitney *U* test.

We show that CVID neutrophils exhibit low surface level of CD16 (Fig. 3). The level of CD16 (Fc γ receptor IIIb; CD16b is the form of CD16 expressed on human neutrophils) increases with neutrophil maturation and serves as a marker of neutrophil differentiation from myelocytes to metamyelocytes, banded neutrophils, and mature segmented neutrophils (48). Low level of neutrophil CD16 is observed in severe bacterial sepsis, infections, and inflammatory states and marks a population of “toxic” or “left-shift” neutrophils with elevated myeloperoxidase activity and

compromised phagocytic and bactericidal activity (49, 50). The level of CD16 is low on neutrophils induced in healthy volunteers following administration of G-CSF (51). The phenotype of neutrophils in CVID patients described in this article is consistent with the phenotype of human G-MDSCs found in the peripheral blood of patients with advanced renal cell carcinoma and pancreatic cancer characterized by low levels of CD16 and CD62L and high levels of CD11b (36, 52). CD16^{low} neutrophils expand in the blood of terminal cancer patients and strongly suppress T cell

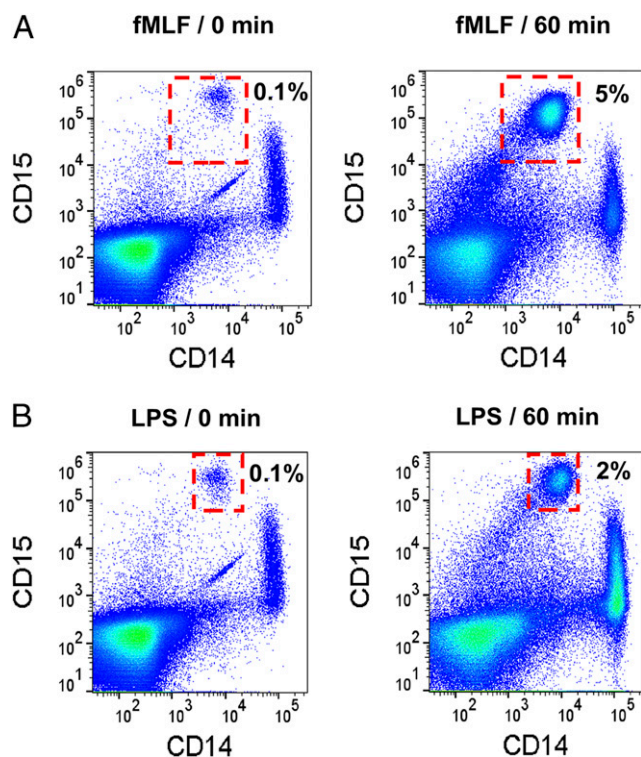


FIGURE 9. Stimulation of whole blood with fMLF or LPS results in an induction of LDNs. Fresh whole blood was either not stimulated or stimulated with fMLF (10 μ M) (A) or LPS (1 μ g/ml) (B) for 60 min. PBMCs were purified by gradient centrifugation, and the frequency of SSC^{high} CCR3⁺ CD14⁺ CD15⁺ LDNs was determined by flow cytometry. Representative data from one of four healthy donors.

proliferation (53). Elegant studies using pulse-chase labeling with 6,6-²H₂-glucose recently demonstrated that CD16^{low} neutrophils represent an immature neutrophil population that is released from the bone marrow several days earlier than mature segmented neutrophils (54). Early mobilization is believed to be a compensatory mechanism allowing the release of substantial numbers of neutrophils, although with lower maturation status and reduced capacity for pathogen clearance (54, 55). The levels of CD16 on CVID neutrophils described in our study closely correlate with the low levels of another myeloid maturation marker CD80 ($r = 0.9$; $p = 0.0008$; Spearman correlation test), consistent with the low maturation status of CD16^{low} cells. Based on these observations, we propose that microbial translocation in CVID patients drives accelerated granulopoiesis and recruitment of alternatively differentiated CD16^{low} neutrophils with potent T cell suppressive activity (19–21, 32).

We demonstrate that CVID is associated with lower neutrophil levels of CD62L (Fig. 2) and that CD62L expression inversely correlates with the level of suppression of T cell proliferation *ex vivo* (Fig. 4). CD62L (L-selectin) mediates the initial tethering and rolling of neutrophils on the endothelial surface. Reduction of CD62L levels can be explained by several distinct mechanisms. CD62L on neutrophils is reduced following administration of G-CSF *in vivo*, and it is shed from the cell surface upon activation with various stimuli, including various bacterial products (56). In this context, we demonstrate that incubation of whole blood with bacterial products fMLF and LPS results in a rapid downmodulation of CD62L on neutrophil surface (Fig. 6). It is, therefore, feasible that CD62L reduction *in vivo* is induced by contact with translocated microbial products. However, an alternative mechanism of the

observed downmodulation of neutrophil CD62L in CVID patients can be postulated. An immune suppressive population of CD62L^{low} neutrophils has been identified following injection of a low dose of LPS in human volunteers (31). This population inhibits T cell function via PD-L1/PD-1 interaction and local release of hydrogen peroxide into the immunological synapse between the neutrophil and T cell (31, 57). Using pulse-chase analysis, authors (54) demonstrated that CD62L^{low} neutrophils with hypersegmented phenotype represent a separate cell population distinct from the banded neutrophils and mature segmented neutrophils. Based on proteome analysis, CD62L^{low} neutrophils are closer to the banded neutrophils than to mature segmented neutrophil population (54). The authors suggest that CD62L^{low} neutrophils represent a distinct subset that enters the bloodstream in response to inflammation. CD62L^{low} neutrophils are not likely to be the reverse-transmigrated neutrophils returning from the tissue back into the bloodstream due to the lack of expression of CD54 or reduced expression of CXCR1 and CXCR2 as determined by flow cytometry (31) and proteomics (54). Low expression of CD62L was also observed in the aged neutrophils subset in mice (46). This subset displayed upregulated CXCR4 receptor. In this study, we have not observed elevated expression of CXCR4 on the CD62L^{low} subset of neutrophils or LDNs in CVID patients. It is feasible that the CD62L^{low} phenotype described here results from a combination of the above-described mechanisms. Recently, a subset of neutrophils in spleen (N_{BH}) with CD62L^{low} CD11b^{hi} phenotype and a tendency to produce NETs has been described (58). N_{BH} display higher expression of CD27, CD40L, CD86, CD95, and HLA-DR and activate Ig production by marginal zone B cells via BAFF, APRIL, and IL-21 (57–62). In addition, several recent reports have indicated the induction of neutrophil–dendritic cell hybrids expressing CD80 and HLA-DR and presenting Ags to CD4⁺ T cells in a variety of models and diseases (63–66). In this study, we have not observed elevated expression of CD80 and HLA-DR on neutrophils from CVID patients. Whether the alteration of neutrophil phenotype directly contributes to the dysregulation of Ig production in CVID patients remains unclear. Future studies should focus on more detailed characterization of a CD62L^{low} population of neutrophils in CVID patients to discern between the alternative mechanisms of downmodulation of CD62L.

CD11b is a marker of degranulation that can be rapidly upregulated on stimulated cells by stimulation with bacterial products, including LPS and fMLF (Fig. 6). In addition, anti-CD3-activated CD8⁺ T cells modulate neutrophil levels of CD11b by IFN- γ production (67). CD11b (complement receptor 3[CR3], MAC-1) is an integrin that forms complexes with CD18 and is stored in secretory, gelatinase, and specific granules (49). Our observation of increased CD11b on CVID neutrophils (Fig. 2) is inconsistent with a previous study (68). The reason for the difference between studies is unclear but can be related to differences in cell processing and staining conditions that may result in different levels of surface CD11b and other markers of degranulation.

We show that CVID patients exhibit an increased frequency of LDNs (Fig. 5). Multiple studies have reported the elevated frequency of LDNs with potent T cell suppressive activity in various inflammatory conditions (30, 34, 36, 37). Although we have not directly addressed the immunosuppressive activity of LDNs in the current study, we report a negative correlation between the frequency of LDNs in PBMCs and intracellular production of IFN- γ by CD8⁺ T cells of CVID patients *ex vivo* ($r = -0.4$; $p = 0.007$). The mechanism of induction of LDNs is currently unclear. As shown in Fig. 9, stimulation of whole

blood with bacterial products fMLF and LPS results in rapid induction of LDNs in the PBMC layer following gradient centrifugation. Thus, it is feasible that LDNs arise from the contact of neutrophils with translocated circulating bacterial products in vivo (11, 12). However, it is unclear whether LDNs induced by ex vivo stimulation are phenotypically identical to those observed in the fresh blood of CVID patients. Overall, the accumulated evidence suggests that low-density phenotype is a cellular property rather than a marker of a specific cell population.

A major mechanism of neutrophil suppression of T cells is the production of ROS (30, 32). Production of ROS and release of arginase can result in downregulation of TCR ζ on T cells, thereby arresting the cells in the G0–G1 phase (32). Our observation that the suppression of T cell activation and production of IFN- γ is ROS-dependent is consistent with previous studies (33, 69). Rapid production of ROS by neutrophils can result in immediate suppression of T cell activation and IFN production. Another potential mechanism of T cell suppression is the upregulation of PD-L1 (Fig. 2) associated with IFN-dependent PD-1-mediated T cell apoptosis (32, 68, 70). The increase of expression of PD-1 on T cells in CVID patients was previously described (9, 10). Although it is feasible that PD-L1/PD-1 interaction contributes to T cell suppression in CVID, we did not observe a correlation between expression of PD-1 on T cells, and enhanced expression of PD-L1 on neutrophils and T cell proliferation was not affected by blocking the PD-L1/PD-1 interaction.

In conclusion, the study presented in this article suggests that neutrophils in CVID patients acquire an altered phenotype and exert potent T cell suppressive activity. The presented results have several limitations, including limited sample size of a cross-sectional study design. Although the data need to be confirmed in future detailed studies employing larger populations, the observations presented in this article provide a qualitatively new view on potential mechanisms of immune suppression in CVID and open new avenues for therapeutic targeting of CVID and other inflammatory disorders.

Disclosures

The authors have no financial conflicts of interest.

References

- Chapel, H., and C. Cunningham-Rundles. 2009. Update in understanding common variable immunodeficiency disorders (CVIDs) and the management of patients with these conditions. *Br. J. Haematol.* 145: 709–727.
- Bogaert, D. J., M. Dullaers, B. N. Lambrecht, K. Y. Vermaelen, E. De Baere, and F. Haerynck. 2016. Genes associated with common variable immunodeficiency: one diagnosis to rule them all? *J. Med. Genet.* 53: 575–590.
- Yazdani, R., M. G. Hakemi, R. Sherkat, V. Homayouni, and R. Farahani. 2014. Genetic defects and the role of helper T-cells in the pathogenesis of common variable immunodeficiency. *Adv. Biomed. Res.* 3: 2.
- Guazzi, V., F. Aiuti, I. Mezzaroma, F. Mazzetta, G. Andolfi, A. Mortellaro, M. Pierdominici, R. Fantini, M. Marziali, and A. Aiuti. 2002. Assessment of thymic output in common variable immunodeficiency patients by evaluation of T cell receptor excision circles. *Clin. Exp. Immunol.* 129: 346–353.
- Vlková, M., V. Thon, M. Sárkyová, L. Bláha, A. Svobodník, J. Lokaj, and J. Litzman. 2006. Age dependency and mutual relations in T and B lymphocyte abnormalities in common variable immunodeficiency patients. *Clin. Exp. Immunol.* 143: 373–379.
- Litzman, J., M. Vlková, Z. Pikulová, D. Stikarovská, and J. Lokaj. 2007. T and B lymphocyte subpopulations and activation/differentiation markers in patients with selective IgA deficiency. *Clin. Exp. Immunol.* 147: 249–254.
- Aspalter, R. M., W. A. Sewell, K. Dolman, J. Farrant, and A. D. Webster. 2000. Deficiency in circulating natural killer (NK) cell subsets in common variable immunodeficiency and X-linked agammaglobulinemia. *Clin. Exp. Immunol.* 121: 506–514.
- Nechvatalova, J., Z. Pikulova, D. Stikarovska, S. Pesak, M. Vlkova, and J. Litzman. 2012. B-lymphocyte subpopulations in patients with selective IgA deficiency. *J. Clin. Immunol.* 32: 441–448.
- Stuchlý, J., V. Kanderová, M. Vlková, I. Heřmanová, L. Slámová, O. Pelák, E. Taraldsrud, D. Jílek, P. Králík Ková, B. Fevang, et al. 2017. Common variable immunodeficiency patients with a phenotypic profile of immunosenescence present with thrombocytopenia. [Published erratum appears in 2017 *Sci. Rep.* 7: 42569.] *Sci. Rep.* 7: 39710.
- Hel, Z., R. P. Huijbregts, J. Xu, J. Nechvatalova, M. Vlkova, and J. Litzman. 2014. Altered serum cytokine signature in common variable immunodeficiency. *J. Clin. Immunol.* 34: 971–978.
- Litzman, J., J. Nechvatalova, J. Xu, O. Ticha, M. Vlkova, and Z. Hel. 2012. Chronic immune activation in common variable immunodeficiency (CVID) is associated with elevated serum levels of soluble CD14 and CD25 but not endotoxaemia. *Clin. Exp. Immunol.* 170: 321–332.
- Barbosa, R. R., S. P. Silva, S. L. Silva, R. Tendeiro, A. C. Melo, E. Pedro, M. P. Barbosa, M. C. Santos, R. M. Victorino, and A. E. Sousa. 2012. Monocyte activation is a feature of common variable immunodeficiency irrespective of plasma lipopolysaccharide levels. *Clin. Exp. Immunol.* 169: 263–272.
- Jørgensen, S. F., M. Trøseid, M. Kummen, J. A. Anmarkrud, A. E. Michelsen, L. T. Osnes, K. Holm, M. L. Høivik, A. Rashidi, C. P. Dahl, et al. 2016. Altered gut microbiota profile in common variable immunodeficiency associates with levels of lipopolysaccharide and markers of systemic immune activation. *Mucosal Immunol.* 9: 1455–1465.
- Amulic, B., C. Cazalet, G. L. Hayes, K. D. Metzler, and A. Zychlinsky. 2012. Neutrophil function: from mechanisms to disease. *Annu. Rev. Immunol.* 30: 459–489.
- Mantovani, A., M. A. Cassatella, C. Costantini, and S. Jaillon. 2011. Neutrophils in the activation and regulation of innate and adaptive immunity. *Nat. Rev. Immunol.* 11: 519–531.
- Mayadas, T. N., X. Cullere, and C. A. Lowell. 2014. The multifaceted functions of neutrophils. *Annu. Rev. Pathol.* 9: 181–218.
- Dancey, J. T., K. A. Deubelbeiss, L. A. Harker, and C. A. Finch. 1976. Neutrophil kinetics in man. *J. Clin. Invest.* 58: 705–715.
- Manz, M. G., and S. Boettcher. 2014. Emergency granulopoiesis. *Nat. Rev. Immunol.* 14: 302–314.
- Boettcher, S., R. C. Gerosa, R. Radpour, J. Bauer, F. Ampenberger, M. Heikenwalder, M. Kopf, and M. G. Manz. 2014. Endothelial cells translate pathogen signals into G-CSF-driven emergency granulopoiesis. *Blood* 124: 1393–1403.
- Boettcher, S., P. Ziegler, M. A. Schmid, H. Takizawa, N. van Rooijen, M. Kopf, M. Heikenwalder, and M. G. Manz. 2012. Cutting edge: LPS-induced emergency myelopoiesis depends on TLR4-expressing nonhematopoietic cells. *J. Immunol.* 188: 5824–5828.
- Casbon, A. J., D. Reynaud, C. Park, E. Khuc, D. D. Gan, K. Schepers, E. Passequé, and Z. Werb. 2015. Invasive breast cancer reprograms early myeloid differentiation in the bone marrow to generate immunosuppressive neutrophils. *Proc. Natl. Acad. Sci. USA* 112: E566–E575.
- Nauseef, W. M., and N. Borregaard. 2014. Neutrophils at work. *Nat. Immunol.* 15: 602–611.
- Scapini, P., O. Marini, C. Tecchio, and M. A. Cassatella. 2016. Human neutrophils in the saga of cellular heterogeneity: insights and open questions. *Immunol. Rev.* 273: 48–60.
- Nicolás-Ávila, J. A., J. M. Adrover, and A. Hidalgo. 2017. Neutrophils in homeostasis, immunity, and cancer. *Immunity* 46: 15–28.
- Tecchio, C., A. Micheletti, and M. A. Cassatella. 2014. Neutrophil-derived cytokines: facts beyond expression. *Front. Immunol.* 5: 508.
- Hotchkiss, R. S., C. M. Coopersmith, J. E. McDunn, and T. A. Ferguson. 2009. The sepsis seesaw: tilting toward immunosuppression. *Nat. Med.* 15: 496–497.
- Chtanova, T., M. Schaeffer, S.-J. Han, G. G. van Dooren, M. Nollmann, P. Herzmark, S. W. Chan, H. Satija, K. Camfield, H. Aaron, et al. 2008. Dynamics of neutrophil migration in lymph nodes during infection. *Immunity* 29: 487–496.
- Beauvillain, C., P. Cunin, A. Doni, M. Scotet, S. Jaillon, M. L. Loiry, G. Magistrelli, K. Masternak, A. Chevaillier, Y. Delneste, and P. Jeannin. 2011. CCR7 is involved in the migration of neutrophils to lymph nodes. *Blood* 117: 1196–1204.
- Müller, I., M. Munder, P. Kropf, and G. M. Hänsch. 2009. Polymorphonuclear neutrophils and T lymphocytes: strange bedfellows or brothers in arms? *Trends Immunol.* 30: 522–530.
- Pillay, J., T. Tak, V. M. Kamp, and L. Koenderman. 2013. Immune suppression by neutrophils and granulocytic myeloid-derived suppressor cells: similarities and differences. *Cell. Mol. Life Sci.* 70: 3813–3827.
- Pillay, J., V. M. Kamp, E. van Hoffen, T. Visser, T. Tak, J. W. Lammers, L. H. Ulfman, L. P. Leenen, P. Pickkers, and L. Koenderman. 2012. A subset of neutrophils in human systemic inflammation inhibits T cell responses through Mac-1. *J. Clin. Invest.* 122: 327–336.
- Leliefeld, P. H., L. Koenderman, and J. Pillay. 2015. How neutrophils shape adaptive immune responses. *Front. Immunol.* 6: 471.
- Bowers, N. L., E. S. Helton, R. P. Huijbregts, P. A. Goepfert, S. L. Heath, and Z. Hel. 2014. Immune suppression by neutrophils in HIV-1 infection: role of PD-L1/PD-1 pathway. *PLoS Pathog.* 10: e1003993.
- Gabrilovich, D. I., and S. Nagaraj. 2009. Myeloid-derived suppressor cells as regulators of the immune system. *Nat. Rev. Immunol.* 9: 162–174.
- Carmona-Rivera, C., and M. J. Kaplan. 2013. Low-density granulocytes: a distinct class of neutrophils in systemic autoimmunity. *Semin. Immunopathol.* 35: 455–463.
- Rodríguez, P. C., M. S. Ernstoff, C. Hernandez, M. Atkins, J. Zabaleta, R. Sierra, and A. C. Ochoa. 2009. Arginase I-producing myeloid-derived suppressor cells in renal cell carcinoma are a subpopulation of activated granulocytes. *Cancer Res.* 69: 1553–1560.
- Eruslanov, E., M. Neuberger, I. Daurkin, G. Q. Perrin, C. Algood, P. Dahm, C. Rosser, J. Vieweg, S. M. Gilbert, and S. Kusmartsev. 2012. Circulating and

- tumor-infiltrating myeloid cell subsets in patients with bladder cancer. *Int. J. Cancer* 130: 1109–1119.
38. Bonilla, F. A., I. Barlan, H. Chapel, B. T. Costa-Carvalho, C. Cunningham-Rundles, M. T. de la Morena, F. J. Espinosa-Rosales, L. Hammarström, S. Nonoyama, I. Quinti, et al. 2016. International consensus document (ICON): common variable immunodeficiency disorders. *J. Allergy Clin. Immunol. Pract.* 4: 38–59.
 39. Malphettes, M., L. Gérard, M. Carmagnat, G. Mouillot, N. Vince, D. Boutboul, A. Bérezné, R. Nove-Josserand, V. Lemoing, L. Tetu, et al; DEFI Study Group. 2009. Late-onset combined immune deficiency: a subset of common variable immunodeficiency with severe T cell defect. *Clin. Infect. Dis.* 49: 1329–1338.
 40. Sandler, N. G., and D. C. Douek. 2012. Microbial translocation in HIV infection: causes, consequences and treatment opportunities. *Nat. Rev. Microbiol.* 10: 655–666.
 41. Hel, Z., J. R. McGhee, and J. Mestecky. 2006. HIV infection: first battle decides the war. *Trends Immunol.* 27: 274–281.
 42. Perreau, M., S. Vigano, F. Bellanger, C. Pellaton, G. Buss, D. Comte, T. Roger, C. Lacabartz, P. A. Bart, Y. Levy, and G. Pantaleo. 2014. Exhaustion of bacteria-specific CD4 T cells and microbial translocation in common variable immunodeficiency disorders. *J. Exp. Med.* 211: 2033–2045.
 43. Bazil, V., and J. L. Strominger. 1991. Shedding as a mechanism of down-modulation of CD14 on stimulated human monocytes. *J. Immunol.* 147: 1567–1574.
 44. Kitchens, R. L., and P. A. Thompson. 2005. Modulatory effects of sCD14 and LBP on LPS-host cell interactions. *J. Endotoxin Res.* 11: 225–229.
 45. Cross, A. S., S. M. Opal, H. S. Warren, J. E. Palardy, K. Glaser, N. A. Parejo, and A. K. Bhattacharjee. 2001. Active immunization with a detoxified *Escherichia coli* J5 lipopolysaccharide group B meningococcal outer membrane protein complex vaccine protects animals from experimental sepsis. *J. Infect. Dis.* 183: 1079–1086.
 46. Zhang, D., G. Chen, D. Manwani, A. Mortha, C. Xu, J. J. Faith, R. D. Burk, Y. Kunisaki, J. E. Jang, C. Scheiermann, et al. 2015. Neutrophil ageing is regulated by the microbiome. *Nature* 525: 528–532.
 47. Pillay, J., I. den Braber, N. Vrsekoop, L. M. Kwast, R. J. de Boer, J. A. Borghans, K. Tesselaar, and L. Koenderman. 2010. In vivo labeling with ²H₂O reveals a human neutrophil lifespan of 5.4 days. *Blood* 116: 625–627.
 48. Elghetany, M. T. 2002. Surface antigen changes during normal neutrophilic development: a critical review. *Blood Cells Mol. Dis.* 28: 260–274.
 49. Kabutomori, O., Y. Iwatani, T. Koh, R. Fushimi, and N. Amino. 1993. Decrease in the density of IgG-Fc receptor III (CD16) on 'toxic' neutrophils. *Acta Haematol.* 89: 163–164.
 50. Hübl, W., S. Andert, G. Thum, S. Ortner, and P. M. Bayer. 1997. Value of neutrophil CD16 expression for detection of left shift and acute-phase response. *Am. J. Clin. Pathol.* 107: 187–196.
 51. Kerst, J. M., M. de Haas, C. E. van der Schoot, I. C. Slaper-Cortenbach, M. Kleijer, A. E. von dem Borne, and R. H. van Oers. 1993. Recombinant granulocyte colony-stimulating factor administration to healthy volunteers: induction of immunophenotypically and functionally altered neutrophils via an effect on myeloid progenitor cells. *Blood* 82: 3265–3272.
 52. Schmielau, J., and O. J. Finn. 2001. Activated granulocytes and granulocyte-derived hydrogen peroxide are the underlying mechanism of suppression of t-cell function in advanced cancer patients. *Cancer Res.* 61: 4756–4760.
 53. Choi, J., B. Suh, Y. O. Ahn, T. M. Kim, J. O. Lee, S. H. Lee, and D. S. Heo. 2012. CD15⁺/CD16^{low} human granulocytes from terminal cancer patients: granulocytic myeloid-derived suppressor cells that have suppressive function. *Tumour Biol.* 33: 121–129.
 54. Tak, T., P. Wijten, M. Heeres, P. Pickkers, A. Scholten, A. J. R. Heck, N. Vrsekoop, L. P. Leenen, J. A. M. Borghans, K. Tesselaar, and L. Koenderman. 2017. Human CD62L^{dim} neutrophils identified as a separate subset by proteome profiling and in vivo pulse-chase labeling. *Blood* 129: 3476–3485.
 55. Glasser, L., and R. L. Fiedlerlein. 1987. Functional differentiation of normal human neutrophils. *Blood* 69: 937–944.
 56. Ohsaka, A., and K. Saionji. 1998. In vivo administration of granulocyte colony-stimulating factor increases the surface expression of sialyl-Lewis(x) on neutrophils in healthy volunteers. *Acta Haematol.* 100: 187–190.
 57. de Kleijn, S., J. D. Langereis, J. Leentjens, M. Kox, M. G. Netea, L. Koenderman, G. Ferwerda, P. Pickkers, and P. W. Hermans. 2013. IFN- γ -stimulated neutrophils suppress lymphocyte proliferation through expression of PD-L1. *PLoS One* 8: e72249.
 58. Chorny, A., S. Casas-Recasens, J. Sintes, M. Shan, N. Polentarutti, R. García-Escudero, A. C. Walland, J. R. Yeiser, L. Cassis, J. Carrillo, et al. 2016. The soluble pattern recognition receptor PTX3 links humoral innate and adaptive immune responses by helping marginal zone B cells. [Published erratum appears in 2017 *J. Exp. Med.* 214: 1559.] *J. Exp. Med.* 213: 2167–2185.
 59. Puga, I., M. Cols, C. M. Barra, B. He, L. Cassis, M. Gentile, L. Comerma, A. Chorny, M. Shan, W. Xu, et al. 2011. B cell-helper neutrophils stimulate the diversification and production of immunoglobulin in the marginal zone of the spleen. *Nat. Immunol.* 13: 170–180.
 60. Gätjen, M., F. Brand, M. Grau, K. Gerlach, R. Kettritz, J. Westermann, I. Anagnostopoulos, P. Lenz, G. Lenz, U. E. Höpken, and A. Rehm. 2016. Splenic marginal zone granulocytes acquire an accentuated neutrophil B-cell helper phenotype in chronic lymphocytic leukemia. *Cancer Res.* 76: 5253–5265.
 61. Parsa, R., H. Lund, A. M. Georgoudaki, X. M. Zhang, A. Ortlieb Guerreiro-Cacais, D. Grommisch, A. Warnecke, A. L. Croxford, M. Jagodic, B. Becher, et al. 2016. BAFF-secreting neutrophils drive plasma cell responses during emergency granulopoiesis. *J. Exp. Med.* 213: 1537–1553.
 62. Deniset, J. F., B. G. Surewaard, W. Y. Lee, and P. Kubes. 2017. Splenic Ly6G^{high} mature and Ly6G^{int} immature neutrophils contribute to eradication of *S. pneumoniae*. *J. Exp. Med.* 214: 1333–1350.
 63. Geng, S., H. Matsushima, T. Okamoto, Y. Yao, R. Lu, and A. Takashima. 2013. Reciprocal regulation of development of neutrophil-dendritic cell hybrids in mice by IL-4 and interferon-gamma. *PLoS One* 8: e82929.
 64. Geng, S., H. Matsushima, T. Okamoto, Y. Yao, R. Lu, K. Page, R. M. Blumenthal, N. L. Ward, T. Miyazaki, and A. Takashima. 2013. Emergence, origin, and function of neutrophil-dendritic cell hybrids in experimentally induced inflammatory lesions in mice. *Blood* 121: 1690–1700.
 65. Singhal, S., P. S. Bhojnarwala, S. O'Brien, E. K. Moon, A. L. Garfall, A. S. Rao, J. G. Quatromoni, T. L. Stephen, L. Litzky, C. Deshpande, et al. 2016. Origin and role of a subset of tumor-associated neutrophils with antigen-presenting cell features in early-stage human lung cancer. *Cancer Cell* 30: 120–135.
 66. Fites, J. S., M. Gui, J. F. Kernien, P. Negoro, Z. Dagher, D. B. Sykes, J. E. Nett, M. K. Mansour, and B. S. Klein. 2018. An unappreciated role for neutrophil-DC hybrids in immunity to invasive fungal infections. *PLoS Pathog.* 14: e1007073.
 67. Pelletier, M., A. Micheletti, and M. A. Cassatella. 2010. Modulation of human neutrophil survival and antigen expression by activated CD4⁺ and CD8⁺ T cells. *J. Leukoc. Biol.* 88: 1163–1170.
 68. Casulli, S., H. Coignard-Biehler, K. Amazzough, M. Shoai-Tehrani, J. Bayry, N. Mahlaoui, C. Elbim, and S. V. Kaveri. 2014. Defective functions of polymorphonuclear neutrophils in patients with common variable immunodeficiency. *Immunol. Res.* 60: 69–76.
 69. Kramer, P. A., L. Prichard, B. Chacko, S. Ravi, E. T. Overton, S. L. Heath, and V. Darley-Usmar. 2015. Inhibition of the lymphocyte metabolic switch by the oxidative burst of human neutrophils. *Clin. Sci. (Lond.)* 129: 489–504.
 70. Hotchkiss, R. S., G. Monneret, and D. Payen. 2013. Sepsis-induced immunosuppression: from cellular dysfunctions to immunotherapy. *Nat. Rev. Immunol.* 13: 862–874.